Transactions of NAS of Azerbaijan, Issue Mathematics, **37** (1), 126–142 (2017).
Series of Physical-Technical and Mathematical Sciences.

Further expansion of the computational horizons for the Green's function modification of the method of functional equations

Yuri A. Melnikov · Volodymyr N. Borodin

Received: 09.09.2016 / Revised: 27.03.2017/ Accepted: 06.04.2017

Abstract. *A specific class of boundary-value problems is targeted for partial differential equations that simulate potential fields induced in thin-wall structures. Computational efficiency is explored for one of the approaches to these problems. It is based on a Green's function modification of the classical method of functional equations proposed by professor Kupradze. The problems are stated in regions of irregular configuration. It is shown that the approach appears workable for a broad range of problems including inverse formulations, which are always extremely expensive computationally. As the key component of the approach, Green's functions are analytically constructed for governing differential equations prior to the actual computer work. This maintains a solid background for fast and accurate solution of direct problems, and creates, consequently, a promising environment for attacking targeted inverse problems.*

Keywords. Potential fields · Thin-wall structures · Green's function method.

Mathematics Subject Classification (2010): 40A20, 65N80

1 Introduction

Construction of Green's functions for applied partial differential equations has been in focus of intensive research in recent decades [3], [4], [9]-[16]. Along with that, Green's functions have been actively incorporated into numerical schemes of the classical boundary integral equation method and its numerous modifications (see, for example, [1], [2], [5], [6], [8], [10]). Extensive database, accumulated so far, explicitly highlights the computational potential of already developed Green's-function-based numerical algorithms. Those algorithms provide high accuracy level attained at a low computational cost in solving various classes of boundary-value problems for partial differential equations applicable in engineering and science.

The present study focuses on a specific class of boundary-value problems for second order partial differential equations. Honoring a trend pioneered in [12] and worked out in some detail in [3], [4], [16], we concentrate on problems simulating potential fields induced in thin shell structures. A semi-analytical approach is advocated here to accurately solve the indicated problem class. The approach is based on the Green's function modification

Y.A. Melnikov
Department of Mathematical Sciences, Computational Sciences Program, Middle Tennessee State University, Murfreesboro, TN 37132, USA,
E-mail: ymelnikov@mtsu.edu

V.N. Borodin
Department of Mechanical Engineering, Tennessee Technological University, Cookeville, TN, 38505, USA
E-mail: vborodin@tntech.edu

[10] of the method of functional equations [7]. Prior to the actual numerical stage of our approach, either closed analytical forms or computer-friendly series containing representations of required Green's functions are obtained for the Laplace equation written in geographical coordinates associated with the middle surface of a given shell. Those functions will be referred to, in the present study, as the *resolving Green's functions*.

A comfortable environment is created with the aid of the described semi-analytical approach. It opens a door into the realm of an important class of inverse problems. In the nowadays engineering and science, inverse problems enjoy a notable demand but are, at the same time, extremely expensive computationally. Extremely high computer cost of inverse problems is predetermined by the nature of the approach that is predominantly used to their solution. The approach is based on the method of successive approximation where a direct problem is supposed to be solved at each single iteration. In this regard, it is worth noting that the number of required iterations might be rather massive counting hundreds and even thousands, explicitly explaining the extreme cost of inverse problems.

The foregoing discussion, makes is clear that the focus in the development of workable algorithms for solution of inverse problems should be on the minimization of computational expense of relevant direct problems. Keeping this in mind, we will turn, in the following section, to resolving Green's functions whose promising computational potential may be exploited to develop an effective approach to direct problems significantly enhancing the productivity of iterative procedures used for solution of inverse problem settings.

2 Construction of resolving Green's functions

labelsec:1 Construction of resolving Green's functions is not a trivial exercise for a specific class of boundary-value problems that we aim at in the present study. Among many factors contributing to the non-triviality of the construction process, the first is geographical coordinates introduced for the considered surface. This makes non-trivial the two-dimensional Laplace equations which govern targeted problems. Such equations are not traditionally encountered in the relevant texts. The second contributing factor is the types of boundary-value problems to be considered. The point is that Dirichlet problems are predominately treated in the well-known Green's-function-related literature. But as to the present work, all the three standard types of boundary conditions (Dirichlet, Neumann, and Robin) could be imposed in the targeted problem statements.

Another important factor, predetermining the non-triviality of the construction procedure for resolving Green's functions, is related to problems set up for assemblies of surfaces. This yields a specific type of boundary-value problems for sets of PDEs each of which is posed in an individual region. The classical Green's function formalism appeared inapplicable to this type of problems and requires a special modification. In order to lay down a basis for that, we had proposed in [11] a workable extension of the Green's function formalism, giving birth to what we call the *matrix of Green's type*.

Prior to addressing the actual treatment of inverse problems (which constitutes the chief objective in the present study), we are going to turn to the complicating factors responsible for the non-triviality in the construction procedures of resolving Green's functions. Our focus in this section is on Green's functions and matrices of Green's type, which will later be required for the development of a suitable background for solution of corresponding direct problems. Following the trend worked out in [11], [12], we will present a number of examples for resolving Green's functions in problems which will later be dealt with on surfaces of revolution and their assemblies.

In order to create a background to the construction of resolving Green's functions, it is convenient to consider a boundary-value problem where the two-dimensional Poisson

equation

$$\nabla^2 u\,(P) = -F\,(P)\,, \qquad P \in \Omega, \tag{2.1}$$

stated in a fragment Ω of a surface, is subject to the boundary condition

$$B[u\,(P)] = 0, \qquad P \in \Lambda \tag{2.2}$$

on a piecewise-smooth contour Λ of Ω.

We assume that the right-hand side function in (2.1) is integrable in Ω, and the boundary-value problem in (2.1) and (2.2) is well-posed. If so then its unique solution can be expressed (see, for example, [6]) in terms of the Green's function $G\,(P;Q)$ of the corresponding to (2.1)–(2.2) homogeneous setting as

$$u\,(P) = \int\int_{\Omega} G\,(P;Q)\,F\,(Q)\,d\Omega\,(Q)\,, \quad P \in \Omega. \tag{2.3}$$

The above assertion will be used, in what follows, as a background for the construction of Green's functions for a number of problems of the type in (2.1)–(2.2) set up on either a single surface fragment or on an assembly of those.

2.1 Spherical fragments

To start with, we focus first on boundary-value problems of the type in (2.1)–(2.2) that simulate potential fields induced in fragments of a spherical surface of radius a. This yields the two-dimensional Poisson equation

$$\frac{1}{a^2 \sin\vartheta}\frac{\partial}{\partial\vartheta}\left(\sin\vartheta\frac{\partial u\,(\vartheta,\varphi)}{\partial\vartheta}\right) + \frac{1}{a^2\sin^2\vartheta}\frac{\partial^2 u\,(\vartheta,\varphi)}{\partial\varphi^2} = -F\,(\vartheta,\varphi) \quad \text{in } \Omega, \tag{2.4}$$

written in geographical coordinates on a sphere of radius a. Let the region Ω represent a fragment of the spherical surface closed in the longitudinal direction φ and bounded with two parallels $\vartheta = \vartheta_0$ and $\vartheta = \vartheta_1$. That is

$$\Omega = \left\{(\vartheta,\varphi) \mid \vartheta_0 \le \vartheta \le \vartheta_1;\ 0 \le \varphi < 2\pi\right\}.$$

This shape will be referred to as the *spherical belt*. Let the solution of the equation in (2.4) be subject to the boundary conditions

$$u\,(\vartheta_0,\varphi) = 0, \qquad \frac{\partial u\,(\vartheta_1,\varphi)}{\partial\vartheta} = 0 \tag{2.5}$$

and

$$u\,(\vartheta,0) = u\,(\vartheta,2\pi)\,, \quad \frac{\partial u\,(\vartheta,0)}{\partial\varphi} = \frac{\partial u\,(\vartheta,2\pi)}{\partial\varphi} \tag{2.6}$$

on the contour of Ω. Clearly, the relations in (2.6) reflect the 2π-periodicity of the problem in the longitudinal direction.

The well-posedness of the problem setting in (2.4)–(2.6) implies the existence of a unique Green's function for the corresponding homogeneous problem.

Clearly, the relation in (2.3) reads, for the setting in (2.4)–(2.6), as

$$u\,(\vartheta,\varphi) = \int_0^{2\pi}\int_{\vartheta_0}^{\vartheta_1} G\,(\vartheta,\varphi;\tau,\psi)\,F\,(\tau,\psi)\,d\Omega\,(\tau,\psi)\,, \quad (\vartheta,\varphi) \in \Omega, \tag{2.7}$$

where the kernel-function $G\,(\vartheta,\varphi;\tau,\psi)$ is supposed to represent the sought-for Green's function of the corresponding to (2.4)–(2.6) homogeneous problem.

Upon implementing the eigenfunction expansion technique, whose description for the considered problems class can, for instance, be found in [12], the Green's function $G(\vartheta,\varphi;\tau,\psi)$ is expressed in the series form

$$G(\vartheta,\varphi;\tau,\psi)=\frac{1}{2}g_0(\vartheta,\tau)+\sum_{n=1}^{\infty}g_n(\vartheta,\tau)\cos n(\varphi-\psi), \tag{2.8}$$

with the coefficient-functions presented as

$$g_0(\vartheta,\tau)=\begin{cases}\ln\frac{\tan\vartheta/2}{\tan\vartheta_0/2}, \vartheta_0\le\vartheta\le\tau\\ \ln\frac{\tan\tau/2}{\tan\vartheta_0/2}, \tau\le\vartheta\le\vartheta_1\end{cases}$$

and

$$g_n(\vartheta,\tau)=\frac{1}{2n\Delta}\begin{cases}\left[\Phi^{2n}(\tau)-\Phi^{2n}(\vartheta_0)\right]\left[\Phi^{2n}(\vartheta_1)+\Phi^{2n}(\vartheta)\right], \vartheta_0\le\vartheta\le\tau\\ \left[\Phi^{2n}(\vartheta)-\Phi^{2n}(\vartheta_0)\right]\left[\Phi^{2n}(\vartheta_1)+\Phi^{2n}(\tau)\right], \tau\le\vartheta\le\vartheta_1\end{cases}$$

where

$$\Delta=\Phi^n(\vartheta)\Phi^n(\tau)\left[\Phi^{2n}(\vartheta_0)+\Phi^{2n}(\vartheta_1)\right] \quad\text{and}\quad \Phi(\gamma)=\tan\gamma/2.$$

Evidently, the series in (2.8) cannot uniformly converge because the Green's function represented by (2.8) possesses the logarithmic singularity. The convergence of the series makes it quite problematic for direct computer implementations. In order to enhance its practical significance, we had suggested (see, for example, [12]) a special transformation aiming at a partial summation of the series and splitting off the singular component of the Green's function. Omitting the summation algebra, we present just the ultimate computer-friendly representation

$$\begin{aligned}G(\vartheta,\varphi;\tau,\psi)=&H\left(\frac{\Phi^2(\vartheta_0)}{\Phi(\vartheta)\Phi(\tau)},\varphi-\psi\right)-H\left(\frac{\Phi(\vartheta)\Phi(\tau)}{\Phi^2(\vartheta_1)},\varphi-\psi\right)\\ &-H\left(\frac{\Phi(\vartheta)}{\Phi(\tau)},\varphi-\psi\right)+H\left(\frac{\Phi^2(\vartheta_0)\Phi(\tau)}{\Phi^2(\vartheta_1)\Phi(\vartheta)},\varphi-\psi\right)\\ &+\frac{1}{2\pi}\ln\frac{\Phi(\vartheta)}{\Phi(\tau)}+R(\vartheta,\varphi;\tau,\psi), \quad \vartheta\le\tau\end{aligned} \tag{2.9}$$

of the sought-for Green's function, where the two-variable function $H(x,y)$ reads as

$$H(x,y)=\frac{1}{4\pi}\ln(1-2x\cos y+x^2).$$

Of the six additive terms in (2.9), the third one represents the logarithmically singular component, whilst the rest of them represent just fragments of its regular component. The last additive term $R(\vartheta,\varphi;\tau,\psi)$ in (2.9) is the fast convergent series

$$R(\vartheta,\varphi;\tau,\psi)=\frac{1}{2\pi}\sum_{n=1}^{\infty}\frac{[\Phi^{2n}(\tau)-\Phi^{2n}(\vartheta_0)][\Phi^{2n}(\vartheta)+\Phi^{2n}(\vartheta_1)]}{n\Phi^{2n}(\vartheta_1)\Phi^n(\vartheta)\Phi^n(\tau)[\Phi^{2n}(\vartheta_0)+\Phi^{2n}(\vartheta_1)]}\cos n(\varphi-\psi).$$

Clearly, the form in (2.9) is valid for $\vartheta\le\tau$. To get the Green's function representation valid for $\tau\le\vartheta$, the variables ϑ and τ in (2.9) should simply be interchanged.

Some of the Green's functions, constructed with the aid of our approach for problems stated on spherical surface, are obtained in closed form containing no series components. That is, for the setting

$$\lim_{\vartheta\to0}|u(\vartheta,\varphi)|<\infty, \quad \left.\frac{\partial u(\vartheta,\varphi)}{\partial\vartheta}\right|_{\vartheta=\pi/2}=0, \quad u(\vartheta,\varphi)|_{\varphi=0,\pi}=0,$$

posed in the fragment $\{0 \le \vartheta \le \pi/2;\ 0 \le \varphi \le \pi\}$, for example, the Green's function is found in the series-less closed analytical form

$$G(\vartheta,\varphi;\tau,\psi) = \frac{1}{4\pi}\left(\ln\frac{\Phi^2(\vartheta) - 2\Phi(\vartheta)\Phi(\tau)\cos(\varphi+\psi) + \Phi^2(\tau)}{\Phi^2(\vartheta) - 2\Phi(\vartheta)\Phi(\tau)\cos(\varphi-\psi) + \Phi^2(\tau)} + \ln\frac{1 - 2\Phi(\vartheta)\Phi(\tau)\cos(\varphi+\psi) + \Phi^2(\vartheta)\Phi^2(\tau)}{1 - 2\Phi(\vartheta)\Phi(\tau)\cos(\varphi-\psi) + \Phi^2(\vartheta)\Phi^2(\tau)}\right),$$

for which the computability is not, of course, an issue.

2.2 A toroidal fragment

To bring another illustration, we turn to a toroidal surface. Consider a circle of radius ρ and a straight line, whose distance from the circle's center is R (with $\rho < R$), belonging to same plane. Let a point (x, y, z) on the toroidal surface, formed by revolving the circle around the line, be determined by the geographical coordinates ϑ (the latitude) and φ (the longitude) as

$$x = D(\vartheta)\cos\varphi, \quad y = D(\vartheta)\sin\varphi, \quad \text{and} \quad z = \rho\cos\vartheta,$$

where $D(\vartheta) = R + a\sin\vartheta$. With the above parametrization in place, the three-dimensional Cartesian Laplace equation reduces to the two-dimensional form

$$\frac{1}{D(\vartheta)}\frac{\partial}{\partial\vartheta}\left(D(\vartheta)\frac{\partial u(\vartheta,\varphi)}{\partial\vartheta}\right) + \frac{\rho^2}{D^2(\vartheta)}\frac{\partial^2 u(\vartheta,\varphi)}{\partial\varphi^2} = 0. \tag{2.10}$$

simulating potential fields induced on the considered toroidal surface.

Let the equation in (2.10) be stated in the fragment $\Omega = \{0 \le \vartheta < 2\pi;\ 0 \le \varphi \le \pi\}$ of the toroidal surface. Clearly, the region Ω is closed in the latitudinal but opened in the longitudinal direction. Impose the Dirichlet conditions

$$u(\vartheta,\varphi)\,|_{\varphi=0} = 0, \qquad u(\vartheta,\varphi)\,|_{\varphi=\pi} = 0 \tag{2.11}$$

on the meridian edges $\varphi = 0$ and $\varphi = \pi$ of Ω, whilst the conditions

$$u(\vartheta,\varphi)\,|_{\vartheta=0} = u(\vartheta,\varphi)\,|_{\vartheta=2\pi}, \quad \left.\frac{\partial u(\vartheta,\varphi)}{\partial\vartheta}\right|_{\vartheta=0} = \left.\frac{\partial u(\vartheta,\varphi)}{\partial\vartheta}\right|_{\vartheta=2\pi} \tag{2.12}$$

are imposed to simulate the fact that the region Ω is closed in the latitudinal direction.

The well-posed boundary-value problem in (2.10)–(2.12) also allows application of the eigenfunction expansion methodology. Omitting details, we just present a closed compact analytical representation of its Green's function $G(\vartheta,\varphi;\tau,\psi)$. It is found ultimately in the form

$$G(\vartheta,\varphi;\tau,\psi) = \frac{1}{4\pi}\ln\frac{\Psi^2(\vartheta) - 2\Psi(\vartheta)\Psi(\tau)\cos(\varphi+\psi) + \Psi^2(\tau)}{\Psi^2(\vartheta) - 2\Psi(\vartheta)\Psi(\tau)\cos(\varphi-\psi) + \Psi^2(\tau)},$$

where

$$\Psi(\gamma) = \exp\left(-\frac{2\pi\rho}{\sqrt{R^2-\rho^2}}\arctan\left(\frac{\rho + R\tan\vartheta/2}{\sqrt{R^2-\rho^2}}\right)\right).$$

2.3 An assembly of surface fragments

A type of problem settings to be analyzed in this section does not fall under the boundary-value problem umbrella in a conventional sense. This creates an environment where the

Green's function formalism does not work, but its recently proposed in [11] extension (with the notion of *matrix of Green's type* introduced) efficiently resolves the situation.

For specificity, let $\Omega = \Omega_1 \cup \Omega_2$ represent an assembly of two fragments of coaxial surfaces of revolution closed in the longitudinal direction. One of them is the hemisphere $\Omega_1 = \{(\vartheta, \varphi)\,|0 \le \vartheta \le \pi/2, 0 \le \varphi < 2\pi\}$ of radius a, whilst another is the toroidal belt $\Omega_2 = \{(\theta, \varphi)\,|\pi/2 \le \theta \le \pi, 0 \le \varphi < 2\pi\}$, with ρ and R staying for the radius of meridian cross-section and the distance from its center to the axis of revolution.

In the compound region Ω, we state the non-conventional boundary-value problem

$$\frac{1}{a^2 \sin\vartheta}\frac{\partial}{\partial\vartheta}\left(\sin\vartheta\frac{\partial u_1(\vartheta,\varphi)}{\partial\vartheta}\right) + \frac{1}{a^2\sin^2\vartheta}\frac{\partial^2 u_1(\vartheta,\varphi)}{\partial\varphi^2} = 0, \quad \text{in } \Omega_1 \tag{2.13}$$

$$\frac{1}{D(\theta)}\frac{\partial}{\partial\theta}\left(D(\theta)\frac{\partial u_2(\theta,\varphi)}{\partial\theta}\right) + \frac{\rho^2}{D^2(\theta)}\frac{\partial^2 u_2(\theta,\varphi)}{\partial\varphi^2} = 0, \quad \text{in } \Omega_2 \tag{2.14}$$

$$\lim_{\vartheta\to 0}|u_1(\vartheta,\varphi)| < \infty, \qquad u_2(\pi,\varphi) = 0 \tag{2.15}$$

$$u_1(\vartheta,0) = u_1(\vartheta,2\pi), \quad \left.\frac{\partial u_1(\vartheta,\varphi)}{\partial\varphi}\right|_{\varphi=0} = \left.\frac{\partial u_1(\vartheta,\varphi)}{\partial\varphi}\right|_{\varphi=2\pi} \tag{2.16}$$

$$u_2(\theta,0) = u_2(\theta,2\pi), \quad \left.\frac{\partial u_2(\theta,\varphi)}{\partial\varphi}\right|_{\varphi=0} = \left.\frac{\partial u_2(\theta,\varphi)}{\partial\varphi}\right|_{\varphi=2\pi} \tag{2.17}$$

and

$$u_1\Big(\frac{\pi}{2},\varphi\Big) = u_2\Big(\frac{\pi}{2},\varphi\Big), \quad \frac{\partial u_1(\pi/2,\varphi)}{\partial\vartheta} = \lambda\frac{\partial u_2(\pi/2,\varphi)}{\partial\theta}, \tag{2.18}$$

where $D(\theta) = R + \rho\sin\theta$ and λ is a positive constant.

Upon implementing the technique proposed in [11], elements of the matrix of Green's type

$$\mathbf{G}(\vartheta,\varphi;\tau,\psi) = (G_{ij}(\vartheta,\varphi;\tau,\psi))_{i,j=1,2}$$

to the problem setting in (2.13)–(2.18) are obtained as

$$\begin{aligned} G_{11}(\vartheta,\varphi;\tau,\psi) = {} & \frac{1}{2\pi}\ln(\Phi(\tau)) + \frac{\sigma_0}{2\pi\Lambda} - H\left(\frac{\Phi(\tau)}{\Phi(\vartheta)},\varphi-\psi\right) \\ & -\frac{\Lambda-1}{\Lambda+1}H\left(\frac{\Phi(\tau)}{\Phi(\vartheta)}e^{2\sigma_0},\varphi-\psi\right) + \frac{\Lambda-1}{\Lambda+1}H(\Phi(\tau)\Phi(\vartheta),\varphi-\psi) \\ & +H\left(\Phi(\tau)\Phi(\vartheta)e^{2\sigma_0},\varphi-\psi\right) + R_{11}(\vartheta,\varphi;\tau,\psi) \end{aligned}$$

$$\begin{aligned} G_{12}(\vartheta,\varphi;\tau,\psi) = {} & \frac{1}{2\pi}\sigma(\pi,\tau) + \frac{2\Lambda}{\Lambda+1}H\left(\Phi(\vartheta)e^{\sigma(\pi/2,\tau)},\varphi-\psi\right) \\ & -\frac{2\Lambda}{\Lambda+1}H\left(\Phi(\vartheta)e^{\sigma(\tau,\pi)+\sigma_0},\varphi-\psi\right) + R_{12}(\vartheta,\varphi;\tau,\psi) \end{aligned}$$

$$\begin{aligned} G_{21}(\theta,\varphi;\tau,\psi) = {} & \frac{1}{2\pi}\sigma(\pi,\theta) - \frac{2}{\Lambda+1}H\left(\Phi(\tau)e^{\sigma(\pi/2,\theta)},\varphi-\psi\right) \\ & +\frac{2}{\Lambda+1}H\left(\Phi(\tau)e^{\sigma(\theta,\pi)+\sigma_0},\varphi-\psi\right) + R_{21}(\theta,\varphi;\tau,\psi) \end{aligned}$$

and

$$G_{22}(\theta,\varphi;\tau,\psi)=\frac{1}{2\pi}\sigma(\theta,\pi)-H\left(e^{\sigma(\tau,\theta)},\varphi-\psi\right)+\frac{\Lambda-1}{\Lambda+1}H\left(e^{\sigma(\tau,\theta)+2\sigma_0},\varphi-\psi\right)$$
$$+H\left(e^{\sigma(\tau,\pi)+\sigma(\theta,\pi)},\varphi-\psi\right)-\frac{\Lambda-1}{\Lambda+1}H\left(e^{\sigma(\pi/2,\theta)+\sigma(\pi/2,\tau)},\varphi-\psi\right)$$
$$+R_{22}(\theta,\varphi;\tau,\psi),$$

where, in addition to the already adapted short-hand notations, we use

$$\sigma(x,y)=\Psi(x)-\Psi(y),\quad \sigma_0=\sigma(\pi/2,\pi),\quad \text{and}\quad \Lambda=\frac{\lambda\rho}{R+\rho}.$$

Remind that the two-variable function $H(x,y)$ has earlier been defined in Section 2, and the series components $R_{ij}=R_{ij}(\vartheta,\varphi;\tau,\psi)$ read as

$$R_{11}=\frac{1}{2\pi}\sum_{n=1}^{\infty}\frac{C_n}{n}\left[e^{n\sigma_0}\left((1-\Lambda)\frac{\Phi^n(\vartheta)}{\Phi^n(\tau)}+(1+\Lambda)\Phi^n(\vartheta)\Phi^n(\tau)\right)\right.$$
$$\left.-e^{-n\sigma_0}\left((1+\Lambda)\frac{\Phi^n(\vartheta)}{\Phi^n(\tau)}+(1-\Lambda)\Phi^n(\vartheta)\Phi^n(\tau)\right)\right]\cos n(\varphi-\psi),$$

$$R_{12}=\frac{\Lambda}{\pi}\sum_{n=1}^{\infty}\frac{C_n}{n}\Phi^n(\vartheta)\sinh n\sigma(\pi,\tau)\cos n(\varphi-\psi),$$

$$R_{21}=\frac{\Lambda}{\pi}\sum_{n=1}^{\infty}\frac{C_n}{n}\Phi^n(\tau)\sinh n\sigma(\pi,\theta)\cos n(\varphi-\psi),$$

$$R_{22}=\frac{1}{\pi}\sum_{n=1}^{\infty}\frac{C_n}{n}\sinh n\sigma(\pi,\tau)\cos n(\varphi-\psi)$$
$$\times\left[(1-\Lambda)e^{n\sigma(\pi/2,\theta)}-(1+\Lambda)e^{n\sigma(\theta,\pi/2)}\right],$$

where

$$C_n=\frac{e^{n\sigma_0}}{(1+\Lambda)^2e^{-2n\sigma_0}-(1-\Lambda^2)}.$$

In physical terms, the $G_{ij}(\vartheta,\varphi;\tau,\psi)$ element of $\mathbf{G}(\vartheta,\varphi;\tau,\psi)$ represents the response of a point $(\vartheta,\varphi)\in\Omega_i$ of Ω to a unit source released at a point $(\tau,\psi)\in\Omega_j$.

Before we jump to the next section, it is worth noting that in the current section we were involved with the construction of Green's functions for problems stated only in regular shape regions.

3 Direct problems in regions of irregular shape

It is absolutely evident that pure analytical methods are irrelevant as to problems stated in irregular shaped regions. Standard numerical methods, like the finite difference or the finite elements could hardly be considered as an alternative either, because of their computational cost, which becomes a decisive factor in inverse problems. That is why semi-analytical approaches come into the play as an option that minimizes the computational cost and maximizes, at the same time, the accuracy level attained. The approach based on the Green's

function modification [10] of the classical functional equation method [7] represents just one of such attractive options.

To illustrate the point, let a triple-connected region Ω on a spherical surface of radius a represent the belt $\{\vartheta_0 \le \vartheta \le \vartheta_1;\ 0 \le \varphi < 2\pi\}$ weakened with an aperture whose contour is a smooth closed line L.

Stated in Ω, we consider the boundary-value problem

$$\frac{1}{a^2 \sin\vartheta}\frac{\partial}{\partial\vartheta}\left(\sin\vartheta\frac{\partial u(\vartheta,\varphi)}{\partial\vartheta}\right)+\frac{1}{a^2\sin^2\vartheta}\frac{\partial^2 u(\vartheta,\varphi)}{\partial\varphi^2}=0,\quad (\vartheta,\varphi)\in\Omega \tag{3.1}$$

$$u(\vartheta,0)=u(\vartheta,2\pi),\quad \frac{\partial u(\vartheta,0)}{\partial\varphi}=\frac{\partial u(\vartheta,2\pi)}{\partial\varphi} \tag{3.2}$$

$$u(\vartheta_0,\varphi)=0,\quad \frac{\partial u(\vartheta_1,\varphi)}{\partial\vartheta}=0 \tag{3.3}$$

and

$$u(\vartheta,\varphi)=U(\vartheta,\varphi),\quad (\vartheta,\varphi)\in L, \tag{3.4}$$

where $U(\vartheta,\varphi)$ is a bounded continuous on L function.

Implementing our procedure (see, for example, [10]) of the Green's function modification of the functional equation method, we express the solution $u(\vartheta,\varphi)$ to (3.1)–(3.4) in the integral form

$$u(\vartheta,\varphi)=\int\limits_{L^*} G(\vartheta,\varphi;\tau,\psi)\,\mu(\tau,\psi)\,dL^*(\tau,\psi),\quad (\vartheta,\varphi)\in\Omega \tag{3.5}$$

where th kernel $G(\vartheta,\varphi;\tau,\psi)$ represents the Green's function to (3.1)–(3.3) set up in the solid spherical belt. The computer-friendly form for $G(\vartheta,\varphi;\tau,\psi)$ was presented in Section 2. As to the line L^* (referred to as the *fictitious contour*), it represents a smooth closed line that is embraced by L, implying L^* is out of Ω.

Evidently, for any integrable on L^* function $\mu(\tau,\psi)$, the integral form in (3.5) represents the exact solution to (3.1) in $\Omega(\vartheta,\varphi)$. The form is also in agreement with the conditions of (3.2) and (3.3). These claims are supported by the defining properties of the resolving Green's function $G(\vartheta,\varphi;\tau,\psi)$. Thus, upon satisfying the boundary condition of (3.4), we arrive at the functional equation

$$U(\vartheta,\varphi)=\int\limits_{L^*} G(\vartheta,\varphi;\tau,\psi)\,\mu(\tau,\psi)\,dL^*(\tau,\psi),\quad (\vartheta,\varphi)\in L \tag{3.6}$$

in the density function $\mu(\tau,\psi)$.

The functional equation in (3.6) is regular, because the sets L and L^* do not share a single point. Hence, a numerical solution of (3.6) is not an issue for a fixed location of the fictitious contour L^*, and approximate values of the density function $\mu(\tau,\psi)$ can be obtained by choosing a set of mesh points on L^* with a subsequent reduction of (3.6) to a well-posed system of linear algebraic equations in approximate values of $\mu(\tau,\psi)$. Once the latter are at hand, the form in (3.5) delivers an approximate analytical solution to the problem in (3.1)–(3.4).

All the above is true for a fixed location and shape of L^*. From our experience it follows that the highest accuracy level in solving a targeted problem could be attained if L^* is a closely located to L line which is either equidistant to it or somewhat close to that. For a circular shape of L, in particular, the optimal shape of L^* appears to be a concentric circle whose radius is within the range $(0.95-0.97)$ of the radius of L.

In order to verify the accuracy level attainable with the proposed approach to the setting in (3.1)–(3.4), we formulate a test problem of this type whose exact solution is at hand. In doing so, we turn to the Green's function $G(\vartheta, \varphi; \tau, \psi)$ of the problem in (3.1)–(3.3) stated in the solid spherical belt $\{\vartheta_0 \le \vartheta \le \vartheta_1;\ 0 \le \varphi < 2\pi\}$. The computer-friendly form of this Green's function has earlier been presented in Section 2 (see equation (2.9)). Evidently, if the source point (τ, ψ) of $G(\vartheta, \varphi; \tau, \psi)$ is arbitrarily fixed at (τ^*, ψ^*) inside of the simply-connected region bounded with L, then the profile $G(\vartheta, \varphi; \tau^*, \psi^*)$ of $G(\vartheta, \varphi; \tau, \psi)$, as a two-variable function of ϑ and φ, represents in Ω the exact solution to (3.1)–(3.4), given that the right-hand side function in (3.4) is the trace of $G(\vartheta, \varphi; \tau^*, \psi^*)$ on L, that is

$$U(\vartheta, \varphi) = G(\vartheta, \varphi; \tau^*, \psi^*), \qquad (\vartheta, \varphi) \in L.$$

Indeed, the suggested location of the source point (τ^*, ψ^*) outside of Ω makes $G(\vartheta, \varphi; \tau^*, \psi^*)$ a solution of the governing equation in Ω, with the boundary conditions of (3.2) and (3.3) satisfied. Subsequently, when the described test problem is solved numerically, the attained accuracy level is entirely under control. In Figure 1, for example, the relative error is presented for the problem in (3.1)–(3.4) where Ω is the spherical cap ($a = 1.0$, $\vartheta_0 = 0.0$, $\vartheta_1 = \pi/3$) weakened with a circular aperture of radius 0.2 centered at $(\pi/6, \pi/2)$.

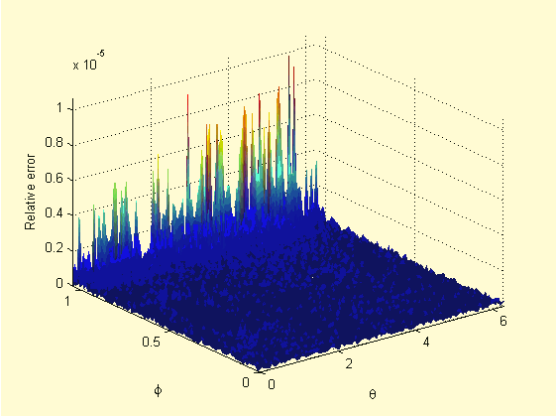

Figure 1. Accuracy level attained in Ω for the test problem.

The accuracy level demonstrated in Figure 1 reveals high computational potential of the technique proposed in this study.

Complexity of the settings that could potentially be treated with our approach will be illustrated by the following example. We turn to the compound reg

ion $\Omega = \Omega_1 \cup \Omega_2$ on a sphere-torus surface composition considered in Section 2. Let the spherical cap Ω_1 be weakened with an aperture whose smooth contour is L. This creates a compound region $\widetilde{\Omega} = \widetilde{\Omega}_1 \cup \Omega_2$, where $\widetilde{\Omega}_1$ is doubly-connected.

The objective in what follows is to develop an efficient procedure for obtaining the matrix of Green's type $\widetilde{\mathbf{G}}(\vartheta, \varphi; \tau, \psi)$ to the boundary-value problem

$$\frac{1}{a^2 \sin\vartheta} \frac{\partial}{\partial \vartheta} \left(\sin\vartheta \frac{\partial u_1(\vartheta, \varphi)}{\partial \vartheta} \right) + \frac{1}{a^2 \sin^2\vartheta} \frac{\partial^2 u_1(\vartheta, \varphi)}{\partial \varphi^2} = 0 \ \text{ in } \widetilde{\Omega}_1, \tag{3.7}$$

$$\frac{1}{D(\theta)} \frac{\partial}{\partial \theta} \left(D(\theta) \frac{\partial u_2(\theta, \varphi)}{\partial \theta} \right) + \frac{\rho^2}{D^2(\theta)} \frac{\partial^2 u_2(\theta, \varphi)}{\partial \varphi^2} = 0, \quad \text{in } \Omega_2, \tag{3.8}$$

$$\lim_{\vartheta\to 0}|u_1(\vartheta,\varphi)|<\infty,\quad u_2(\pi,\varphi)=0, \tag{3.9}$$

$$u_i(\vartheta,0)=u_i(\vartheta,2\pi),\quad \left.\frac{\partial u_i(\vartheta,\varphi)}{\partial\varphi}\right|_{\varphi=0}=\left.\frac{\partial u_i(\vartheta,\varphi)}{\partial\varphi}\right|_{\varphi=2\pi},\quad i=1,2, \tag{3.10}$$

$$u_1\Big(\frac{\pi}{2},\varphi\Big)=u_2\Big(\frac{\pi}{2},\varphi\Big),\quad \frac{\partial u_1(\pi/2,\varphi)}{\partial\vartheta}=\lambda\frac{\partial u_2(\pi/2,\varphi)}{\partial\theta} \tag{3.11}$$

and

$$u_1(\vartheta,\varphi)=0,\quad (\vartheta,\varphi)\in L \tag{3.12}$$

set up in $\widetilde{\Omega}=\widetilde{\Omega}_1\cup\Omega_2$.

Clearly, the irregularity of the shape of $\widetilde{\Omega}$ and its compound structure are the biggest obstacles in reaching the stated objective. The matrix of Green's type extension allows however to overcome these obstacles.

In order to obtain the elements of $\widetilde{\mathbf{G}}(\vartheta,\varphi;\tau,\psi)$ in compliance with our approach, a resolving matrix of Green's type is required. The matrix $\mathbf{G}(\vartheta,\varphi;\tau,\psi)$ constructed in Section 2 will be chosen as such. It allows the targeted matrix $\widetilde{\mathbf{G}}(\vartheta,\varphi;\tau,\psi)$ to be expressed in terms of $\mathbf{G}(\vartheta,\varphi;\tau,\psi)$ in the form

$$\widetilde{\mathbf{G}}(\vartheta,\varphi;\tau,\psi)=\mathbf{G}(\vartheta,\varphi;\tau,\psi)+\mathbf{W}^*(\vartheta,\varphi) \tag{3.13}$$

where the two-by-two corrector-matrix $\mathbf{W}^*(\vartheta,\varphi)$ is expressed as

$$\mathbf{W}^*(\vartheta,\varphi)=\begin{pmatrix} w_{11}^*(\vartheta,\varphi) & 0\\ w_{21}^*(\theta,\varphi) & 0\end{pmatrix}.$$

The elements $w_{11}^*(\vartheta,\varphi)$ and $w_{21}^*(\vartheta,\varphi)$ of $\mathbf{W}^*(\vartheta,\varphi)$ can be expressed in terms of the first column elements of the resolving matrix $\mathbf{G}(\vartheta,\varphi;\tau,\psi)$ as

$$w_{11}^*(\vartheta,\varphi)=\int\limits_{L_0}G_{11}(\vartheta,\varphi;\tau,\psi)\,\mu_1^*(\tau,\psi)\,dL_0(\tau,\psi),\quad (\vartheta,\varphi)\in\Omega_1 \tag{3.14}$$

and

$$w_{21}^*(\theta,\varphi)=\int\limits_{L_0}G_{21}(\theta,\varphi;\tau,\psi)\,\mu_1^*(\tau,\psi)\,dL_0(\tau,\psi),\quad (\theta,\varphi)\in\Omega_2,$$

where L_0 represents a fictitious contour.

Taking the limit in (3.14) as the field point (ϑ,φ) approaches the actual contour L of the aperture, we arrive, in view of the boundary condition of (3.12) and the form of $\widetilde{\mathbf{G}}(\vartheta,\varphi;\tau,\psi)$ in (3.13), at the regular functional equation

$$\int\limits_{L_0}G_{11}(\vartheta,\varphi;\tau,\psi)\,\mu_1^*(\tau,\psi)\,dL_0(\tau,\psi)=-G_{11}(\vartheta,\varphi;\tau^*,\psi^*),\quad (\vartheta,\varphi)\in L \tag{3.15}$$

in the density function $\mu_1^*(\tau,\psi)$.

The efficiency of the proposed approach is verified in Figure 2, where a potential field induced by multiple point sources in the considered perforated spherical-toroidal joint structure. The field was computed within the scope of the described numerical procedure.

The geometry of the considered joint structure is defined with the parameters: $a=0.6$, $\rho=0.7$, $\vartheta_0=0.0$, $\vartheta_1=\pi/2$, $\theta_0=\pi/2$, $\theta_1=\pi$, and $R=1.3$. The unit point sources are placed at $(0.33\pi,0.24\pi)$ in the spherical fragment, and $(0.58\pi,0.52\pi)$ and $(0.68\pi,0.28\pi)$ in the toroidal fragment. The circular aperture of radius 0.2 is centered at $(0.35\pi,0.5\pi)$ in the spherical fragment.

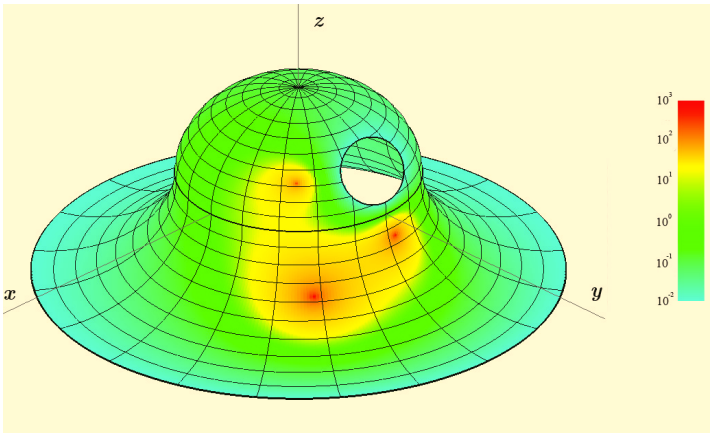

Figure 2. Potential field induced by multiple sources in the joint structure.

4 Inverse problems

The discussion that we held in the previous sections has laid a solid foundation for the basic study in the present work. Namely, some persuasive arguments will be presented, in what follows, to verify the efficiency of our approach to inverse problems. A number of inverse formulations will be treated for problem settings that arise while investigating potential fields in various thin shell structures of irregular configuration.

To start with, we turn to the direct boundary-value problem (3.1)–(3.4) considered earlier in Section 3. The problem is stated in the triple-connected region Ω on a spherical surface of radius a, which represents the belt $\{\vartheta_0 \leq \vartheta \leq \vartheta_1;\ 0 \leq \varphi < 2\pi\}$ weakened with an aperture whose contour L is determined by intersection of the spherical surface with a cylinder of radius r whose axis passes through the point $(\vartheta_c, 0)$ on the spherical surface and the surface center. Let $u(\vartheta, \varphi)$ represent the solution to this direct problem. In physical terms, the problem could be interpreted as simulating a steady-state heat conduction process in a thin shell for which Ω represents the middle surface. The edges $\vartheta = \vartheta_0$ and $\vartheta = \vartheta_1$ of the shell are kept at zero temperature and zero heat flux, respectively, whilst the contour L is kept at temperature $U(\vartheta, \varphi)$.

We are going to turn now to an inverse formulation of the problem in (3.1)–(3.4) by assuming that a few of its defining parameters are missing and ought to be restored in order to meet some constraints imposed on the solution that we are looking for. To be specific, let the size and the shape of the spherical belt be fixed (implying the parameters $a,\ \vartheta_0$, and ϑ_1 are given). Let also the function $U(\vartheta, \varphi)$ in (3.4) be fixed. Given all the above, we aim at determining the location and size of the aperture (the values of r and ϑ_c are to find) for which the following constraints

$$\max_{\vartheta=\vartheta_0} u(\vartheta, \varphi) \leq C \quad \text{and} \quad \max_{\vartheta=\vartheta_1} \frac{\partial u(\vartheta, \varphi)}{\partial \vartheta} \leq D \tag{4.1}$$

hold, with C and D being fixed positive constants.

The just described inverse formulation is not, of course, well-posed. Indeed, it is quite possible that, for a given set of the defining parameters, the problem might either have no solution complying with (4.1) or allows multiple solutions. To clearly underline the focus of our work, note that the existence and uniqueness issues are left aside, and we just concentrate on the search of a single feasible solution (if any) of the inverse formulation, for

a fixed set of the defining parameters. Such a pragmatic approach is customarily accepted in engineering practice.

Our strategy of handling the described inverse problem is based on an iterative implementation of the efficient Green's-function-based algorithm (which was actually presented and justified in Section 3) to the direct problem in (3.1)–(3.4). In following this strategy, the solution of the described inverse problem reduces to the system of non-linear equations

$$\begin{aligned} f_1(r, \vartheta_c) &= C \\ f_2(r, \vartheta_c) &= D \end{aligned} \tag{4.2}$$

in r and ϑ_c, where

$$f_1(r, \vartheta_c) \equiv \max u(\vartheta_0, \varphi) \quad \text{and} \quad f_2(r, \vartheta_c) \equiv \max \frac{\partial u(\vartheta_1, \varphi)}{\partial \vartheta}.$$

The intricate point of the above system is that both functions $f_1(r, \vartheta_c)$ and $f_2(r, \vartheta_c)$ depend on their arguments implicitly. Hence, the standard techniques are problematic to directly apply. However, after studying the behavior of the functions $f_1(r, \vartheta_c)$ and $f_2(r, \vartheta_c)$, we discovered their remarkable properties that are very suggestive in the development of our strategy. That is, both of these functions increase if the variable r increases, whereas $f_1(r, \vartheta_c)$ decreases whilst $f_2(r, \vartheta_c)$ increases if the variable ϑ_c increases.

These properties allow us to use the following instruments in the iterative procedure to achieve an appropriate approximate solution of the system in (4.2):

a) to increase both $f_1(r, \vartheta_c)$ and $f_2(r, \vartheta_c)$, we increment the value of r,

b) to increase $f_1(r, \vartheta_c)$ and decrease $f_2(r, \vartheta_c)$, we decrement the value of ϑ_c,

c) to decrease $f_1(r, \vartheta_c)$ and increase $f_2(r, \vartheta_c)$, the value of ϑ_c should go up,

and

d) if both $f_1(r, \vartheta_c)$ and $f_2(r, \vartheta_c)$ must decrease, then the value of r goes down.

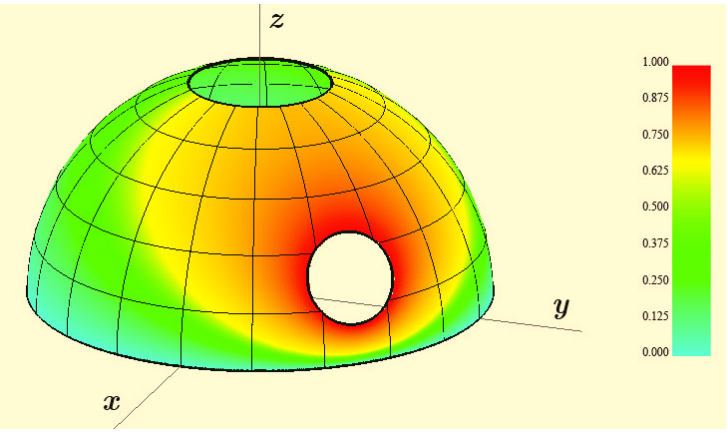

Figure 3. Solution of the inverse problem for the spherical belt with aperture.

The recovered solution of the inverse problem stated in this section is shown in Figure 3, with the parameters determining its statement chosen as $a = 1.0$, $\vartheta_0 = 0.1\pi$, $\vartheta_1 = 0.5\pi$, $U \equiv 1.0$, $C = 0.85$, $D = 10.0$. The approximate values for the targeted parameters were found as $r \approx 0.2011$, $\vartheta_c \approx 1.1938$. It took a few dozens of iterations to attain the accuracy level of order 10^{-4} for both parameters C and D. Note that the iterative process was started with the initial parameter values of $r = 0.05$ and $\vartheta_c = 0.2\pi$.

In order to formulate another inverse problem, we turn back to the equations in (3.7) and (3.8) from Section 3. Let $\widetilde{\Omega}_1$ in (3.7) be a double-connected region representing the quadrilateral $\{(\vartheta,\varphi)\,|\vartheta_0 \le \vartheta \le \vartheta_1, 0 \le \varphi \le \pi/2\}$ on a spherical surface of radius a weakened with a circular aperture whose contour L of radius r_c is centered at (ϑ_c,φ_c). Let Ω_2 in (3.8) represent a quadrilateral region $\{(\theta,\varphi)\,|\theta_0 \le \theta \le \theta_1, 0 \le \varphi \le \pi/2\}$ on a toroidal surface of radii R and ρ. Let the regions $\widetilde{\Omega}_1$ and Ω_2 contact each other along the line $\vartheta_1 = \theta_0$ forming the compound region $\widetilde{\Omega} = \widetilde{\Omega}_1 \cup \Omega_2$.

In $\widetilde{\Omega}$, we consider the boundary value problem

$$u_1(\vartheta_0,\varphi) = 0, \quad u_2(\theta_1,\varphi) = 0, \tag{4.3}$$

$$u_1(\vartheta,0) = u_1\left(\vartheta,\frac{\pi}{2}\right) = 0, \quad u_2(\theta,0) = u_2\left(\theta,\frac{\pi}{2}\right) = 0, \tag{4.4}$$

$$u_1(\vartheta_1,\varphi) = u_2(\theta_0,\varphi), \quad \frac{\partial u_1(\vartheta_1,\varphi)}{\partial\vartheta} = \lambda\frac{\partial u_2(\theta_0,\varphi)}{\partial\theta}, \tag{4.5}$$

and

$$u_1(\vartheta,\varphi) = U(\vartheta,\varphi), \quad (\vartheta,\varphi) \in L. \tag{4.6}$$

for equations (3.7) and (3.8). The right-hand side $U(\vartheta,\varphi)$ in (4.6) is supposed to be integrable on L function.

For the inverse formulation of the problem in (3.7), (3.8), (4.3)–(4.6), we aim at determining a location and a size of the aperture, along with a positive parameter λ in (4.5), to meet the following constraining criteria

$$\int_0^{\pi/2}\frac{\partial u_1(\vartheta_0,\varphi)}{\partial\vartheta}d\varphi \le A, \quad \int_0^{\pi/2}\frac{\partial u_2(\theta_1,\varphi)}{\partial\theta}d\varphi \le B,$$

$$\int_{\vartheta_0}^{\vartheta_1}\frac{\partial u_1(\vartheta,0)}{\partial\varphi}d\vartheta + \int_{\theta_0}^{\theta_1}\frac{\partial u_2(\theta,0)}{\partial\varphi}d\theta \le C,$$

$$\int_{\vartheta_0}^{\vartheta_1}\frac{\partial u_1(\vartheta,\pi/2)}{\partial\varphi}d\vartheta + \int_{\theta_0}^{\theta_1}\frac{\partial u_1(\theta,\pi/2)}{\partial\varphi}d\theta \le D,$$

where $A,\ B,\ C$, and D are fixed positive parameters. So, the parameters $\vartheta_c,\ \varphi_c,\ r_c$, and λ are to be determined. The rest of the geometrical parameters determining the problem statement are supposed to be fixed.

An iterative procedure, similar to that implemented for the previous inverse problem, was developed and applied for the current statement as well. Required for solution of the direct problem resolving matrix represents, in this case, the matrix of Green's type to the problem in (3.7), (3.8), (4.3)–(4.5).

The procedure was applied to the problem in (3.7), (3.8), (4.3)–(4.6), where the shape of $\widetilde{\Omega}$ is determined with the following parameters: $a = 3.5$, $\rho = 1.4$, $\vartheta_0 = \pi/5$, $\vartheta_1 = \pi/2$, $\theta_0 = 0.6\pi$, $\theta_1 = 1.2\pi$, and $R = a\sin(\vartheta_1) + \rho\sin(\theta_0) \approx 4.831$. The parameters specifying the constrainig criteria were fixed as: $A = 3.0$, $B = 0.1$, $C = 1.0$, and $D = 2.0$. The iterative procedure has been launched with initial values of the sought-for parameters chosen as: $\vartheta_c = 0.8$, $\varphi_c = 0.3$, $r_c = 0.35$, and $\lambda = 1.0$. It took around 40 iterations to attain the accuracy level of 10^{-4} for all four parameters. The ultimate values of the sought-for parameters were found as: $\vartheta_c \approx 1.1909$, $\varphi_c \approx 0.9047$, $r_c \approx 0.8787$, and $\lambda \approx 22.018$. The ultimate potential field in the optimally shaped compound structure is shown in Figure 4.

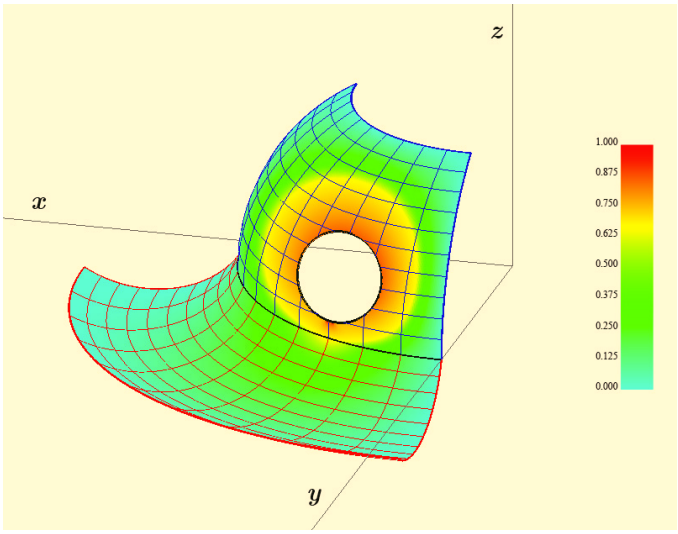

Figure 4. Solution of the inverse problem in the compound structure with aperture.

Concluding the discussion, we turn to another potential problem stated in a compound surface structure, and formulate it in physical terms. Let a compound thin spherical shell of radius a consist of two congruent fragments whose middle surfaces occupy the regions $\Omega_1 = \{0 \le \vartheta \le \pi/2;\ 0 \le \varphi \le \pi/2\}$ and $\Omega_2 = \{\pi/2 \le \vartheta \le \pi;\ 0 \le \varphi \le \pi/2\}$. Let the fragments be made of different conductive materials, with λ representing their relative coefficient of conductivity. Let also the fragment Ω_1 contain a circular aperture L of radius r_c centered at (ϑ_c, φ_c), forming the double-connected region $\widetilde{\Omega}_1$. A potential field will be analyzed as induced by a point source of intensity E released at a point (τ_s, ψ_s) in fragment Ω_2. To be specific, we formulate the following boundary-value problem

$$\frac{1}{a^2 \sin\vartheta}\frac{\partial}{\partial\vartheta}\left(\sin\vartheta\frac{\partial u_1(\vartheta,\varphi)}{\partial\vartheta}\right) + \frac{1}{a^2\sin^2\vartheta}\frac{\partial^2 u_1(\vartheta,\varphi)}{\partial\varphi^2} = 0 \quad \text{in } \widetilde{\Omega}_1, \tag{4.7}$$

$$\frac{1}{a^2 \sin\vartheta}\frac{\partial}{\partial\vartheta}\left(\sin\vartheta\frac{\partial u_2(\vartheta,\varphi)}{\partial\vartheta}\right) + \frac{1}{a^2\sin^2\vartheta}\frac{\partial^2 u_2(\vartheta,\varphi)}{\partial\varphi^2} = -E\delta(\tau_s,\psi_s) \quad \text{in } \Omega_2, \tag{4.8}$$

$$\lim_{\vartheta\to 0}|u_1(\vartheta,\varphi)| < \infty, \quad \lim_{\vartheta\to\pi}|u_2(\vartheta,\varphi)| < \infty, \tag{4.9}$$

$$u_1(\vartheta,0) = u_2(\vartheta,0) = 0, \quad \frac{\partial u_1(\vartheta,\pi/2)}{\partial\varphi} = \frac{\partial u_2(\vartheta,\pi/2)}{\partial\varphi} = 0, \tag{4.10}$$

$$u_1\left(\frac{\pi}{2},\varphi\right) = u_2\left(\frac{\pi}{2},\varphi\right), \quad \frac{\partial u_1(\pi/2,\varphi)}{\partial\vartheta} = \lambda\frac{\partial u_2(\pi/2,\varphi)}{\partial\vartheta}, \tag{4.11}$$

and

$$u_1(\vartheta,\varphi) = 0, \quad (\vartheta,\varphi) \in L \tag{4.12}$$

in the compound region $\widetilde{\Omega} = \widetilde{\Omega}_1 \cup \Omega_2$ of irregular shape, where the right-hand side of equation in (4.8) is expressed in terms of the Dirac Delta function.

The Green's function modification of the functional equation method, which we advocated in Section 3, appears also productive in solving the direct problem in (4.7)–(4.12). As an illustration, we depicted in Figure 5 the potential field induced in $\widetilde{\Omega}$ with the following values of the problem defining parameters: $a = 1.5$, $r_c = 0.3$, $\vartheta_c = 0.3\pi$, $\varphi_c = 0.3\pi$, $\tau_s = 0.575\pi$, $\psi_s = 0.375\pi$, $E = 2.4$, and $\lambda = 0.1$.

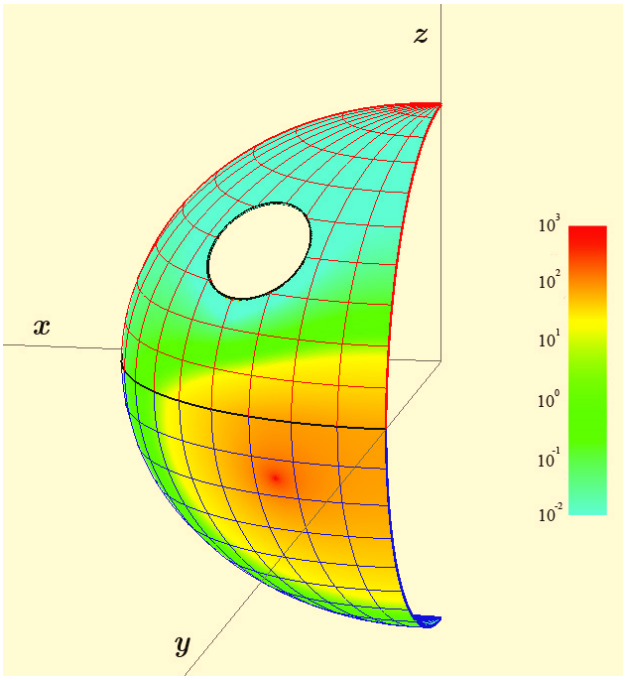

Figure 5. Solution of a direct problem for the composed spherical shell.

As an example of inverse formulation for the problem in (4.7)–(4.12), let us assume that all its defining parameters, except for λ, are fixed as shown above, and we aim at the recovering a value of λ that holds the contour integral

$$\int_L \frac{\partial u\left(\vartheta,\varphi\right)}{\partial \mathbf{n}}\, dL$$

at a minimal possible level. This inverse problem setting reflects the energy saving strategy in keeping the potential on L at zero level.

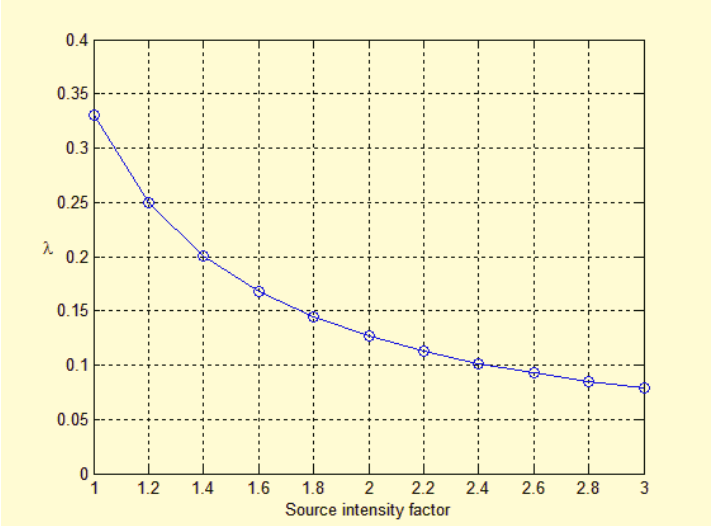

Figure 6. Relation between E and λ revealed for the inverse problem.

Quite frequently in engineering reality, time consuming computational experiments are required. Note that the computational efficiency of our approach creats a strong basis for such an experimental work. For the just discussed inverse problem, for example, we have conducted one of those experiments, revealing, in Figure 6, the relation between the parameters E and λ.

5 Concluding remarks

The data presented and discussed in this study build up a confidence in the Green's function modification of the functional equation method that we have applied to a broad variety of problems set up in multiply-connected irregular shaped regions for elliptic equations whose coefficients might be defined in a piecewise fashion. The most remarkable feature, that makes our approach efficient computationally, is the use of resolving Green's functions or matrices of Green's type, which are obtained analytically prior to actual numerical work, radically enhancing the overall potential of our approach. As the result, the required computer time radically decreases compared to other traditional approaches of the classical boundary integral equation method. This creates, subsequently, a workable environment that allows to practically tackle even inverse problem statements.

References

1. Banerjee, P.K., Batterfield, R.: Boundary Element Method in Engineering Science, 452. *McGraw Hill, London* (1981).
2. Bogomolny, A.: *Fundamental solutions method for elliptic boundary-value problems*, SIAM Journal on Numerical Analysis, **22**, 644-669 (1985).
3. Borodin, V.N.: *A semi-analytical approach to Green's functions for problems in multiply-connected regions on a spherical surface*, Journal of Mathematics and System Science, **3** (12), 597–601 (2013).
4. Borodin, V.N., Melnikov, Y.A.: *Potential fields induced by point sources in assemblies of thin shells weakened with apertures*, Mathematical Methods in the Applied Sciences, **38** (8), 1472–1484 (2015).
5. Brebbia, C.A.: The Boundary Element Method for Engineers, 196. *Pentech Press, Halstead Press, London - New York* (1978).
6. Courant, A., Hilbert, D.: Methods of Mathematical Physics, 560. *Interscience, New York* (1953).
7. Kupradze, V.D., Aleksidze, M.A.: *The method of functional equations for the approximate solution of certain boundary-value problems*, USSR Computational Mathematics and Mathematical Physics, **4**, 82–126 (1964).
8. Kupradze, V.D.: Potential Method in the Theory of Elasticity, 339. *Davey, New York* (1965).
9. Lifanov, I.K., Melnikov, Y.A., Nenashev, A.S.: *Green's functions for regions of irregular shape and singular integral equations*, Doklady Rosijskoj Akademii Nauk, **410** (3), 313–317 (2006).
10. Melnikov, Y.A.: *Some applications of the Green's function method in mechanics*, International Journal of Solids and Structures, **13**, 1045–1058 (1977).
11. Melnikov, Y.A.: *Green's function formalism extended to systems of mechanical differential equation posed on graphs*, Journal of Engineering Mathematics, **34** (3), 369–386 (1998).
12. Melnikov, Y.A.: Influence Functions and Matrices, 469. *Marcel Dekker, New York - Basel* (1999).

13. Melnikov, Y.A.: *Efficient representations of Green's functions for some elliptic equations with piecewise-constant coefficients*, Central European Journal of Mathematics, **8** (1), 53–72 (2010).
14. Melnikov, Y.A., Melnikov, M.Y.: Green's Functions: Construction and Applications, 440. *DeGruyter, Berlin - Boston* (2012).
15. Melnikov, Y.A.: *To the efficiency of a Green's function modification of the method of functional equations*, Journal of Applied and Computational Mathematics, **3** (3), 1–7 (2014).
16. Melnikov, Y.A., Borodin, V.N.: Green's Functions. Potential Fields on Surfaces, 195. *Springer Birkhauser, New York - London* (2017).